Isothermal CO_2 Gasification Reactivity and Kinetic Models of Biomass Char/Anthracite Char

Hai-Bin Zuo,[a,*] Peng-Cheng Zhang,[a] Jian-Liang Zhang,[a,b,*] Xiao-Tao Bi,[c] Wei-Wei Geng,[a] and Guang-Wei Wang[b]

Gasification of four biomass chars and anthracite char were investigated under a CO_2 atmosphere using a thermo-gravimetric analyzer. Reactivity differences of chars were considered in terms of pyrolysis temperature, char types, crystallinity, and inherent minerals. The results show that the gasification reactivity of char decreased with the increase of pyrolysis temperature. Char gasification reactivity followed the order of anthracite coal char (AC-char) < pine sawdust char (PS-char) < peanut hull char (PH-char) < wheat straw char (WS-char) < corncob char (CB-char) under the same pyrolysis temperature. Two repesentative gas-solid models, the random pore model (RPM) and the modified random pore model (MRPM), were applied to describe the reactive behaviour of chars. The results indicate RPM performs well to describe gasification rates of chars but cannot predict the phenomenon that there appears to exist a peak conversion for biomass chars at a high conversion rate, where the MRPM performs better.

Keywords: Anthracite char; Biomass char; Gasification; Kinetic model; RPM; MRPM

Contact information: a: State Key Laboratory of Advanced Metallurgy, University of Science and Technology Beijing, Beijing 100083, China; b: School of Metallurgical and Ecological Engineering, University of Science and Technology Beijing, Beijing 100083, China; c: Chemical and Biological Engineering, University of British Columbia, Vancouver, V6T 1Z3 Canada;
** Corresponding author: zuohaibin@ustb.edu.cn; zhang.jianliang@hotmail.com*

INTRODUCTION

Energy and the related environmental crisis have been the most challenging problem in the world for the past decades. With the growth of economic activity, the enormous consumption of fossil fuels has caused serious environmental contamination and damage to ecological systems. Meanwhile being the major components of the current energy supply, coal, crude oil, and natural gas are also precious organic chemical raw materials; excessive consumption will accelerate their depletion because they are non-renewable. Therefore, recent studies have been focusing on replacing the traditional fossil fuels with renewable and environmental friendly energies (Demirbas 2005; Wang *et al.* 2014). Among various kinds of renewable energy, biomass energy is considered a clean energy due to its carbon neutral nature and its massive amount, wide distribution, and huge exploitation potential. Hence, biomass energy will become one of the most important and promising energy supplies in the world. China is very rich in various biomass resources. Approximately 1.32 billion tons of biomass, such as agricultural and forestry residues, can be used as an energy source every year. Replacing fossil fuel with biomass energy can alleviate the energy crisis, and also reduce air contamination, as well as green-house gas emission, which is consistent with the trend of a global low carbon economy.

Unlike traditional fossil fuels, such as coal, biomass energy is characterized as

having low energy density and high moisture/volatile matter content. These characteristics of raw biomass varieties make them difficult to be used in industrial production directly, whether it be as reducing agent, fuel, or other applications. Thus, the necessary transformation treatments have to be executed before the biomass is utilized. These treatments commonly refer to the thermochemical conversion processes, such as combustion, gasification, carbonization, and liquefaction (McKendry 2002b; Chouchene *et al.* 2012; Dorge *et al.* 2011; Jeong *et al.* 2014; Masnadi *et al.* 2014). Biomass gasification is one of the most promising technologies, because of its ability to rapidly convert large amounts and various kinds of biomass into easily storable and transportable gas, liquid fuel, or solid products (Barea *et al.* 2009). Generally speaking, the gasification processes in a gasifier consist of water evaporation, volatiles pyrolysis, combustion, volatiles gasification, and char gasification. Some processes overlap and interact, so it is very complex. Among theses processes, char gasification is the controlling step due to its low gasifcation rate. In addition, the char-CO_2 gasification rate is much lower than the steam gasification rate of chars. It follows that the char-CO_2 gasification rate is regarded as the rate-determining step in practical gasification process. As a result, investigation on the reaction behavior of char-CO_2 gasification and kinetic parameters of gasfication stage can provide a basic foundation for better understanding the reaction mechanism and optimizing design of reactor design for the biomass gasification production (Wu *et al.* 2006). There are many references dealing with the kinetics of the gasification of biomass chars. Many researchers have performed experimental studies on gasification in steam atmosphere with various feedstocks (Rapagna *et al.* 2000; Huo *et al.* 2014; Gunarathne *et al.* 2014; Hognon *et al.* 2014), whereas many authors have studied gasification processes in CO_2 atmosphere using a thermogravimetric analyser (Ahn *et al.* 2001; Zou *et al.* 2007; Mani *et al.* 2011; Wang *et al.* 2014). Currently, various kinetic models have been extensively employed for the investigations regarding the gasification performance of biomass char at CO_2 atmosphere. It is noted, however, that most studies have centered on the synthesis of biomass char at relatively low temperatures as opposed to high temperatures (Chen *et al.* 2013; Richardson *et al.* 2015). Moreover, those factors imposing an impact on the gasification have failed to be fully considered. Therefore, it is of critical importance to ascertain the gasification of biomass char at high temperatures, meanwhile providing the theoretical basis for utilization of biomass more efficiently.

The purpose of the present study was to investigate the reactivity of four typical biomass chars and one anthracite char with CO_2, through thermo-gravimetric analysis (TGA); the gasification reaction kinetics data were then analyzed using the Random Pore model (RPM), which was introduced in the analysis of char gasification kinetics based on experimental data. Kinetic parameters of the gasification process were ascertained, offering a theoretical reference for proper design, construction, and operation of gasifiers as well as a process scale-up for char gasification. It is anticipated that this study will be useful in providing reference information and a theoretical basis for the efficient use of biomass in China.

EXPERIMENTAL

Fuel Samples

One typical anthracite coal (AC) from Hebei province in China and four representative agricultural and forestry wastes, pine sawdust (PS), wheat straw (WS), corncob (CB), and peanut hull (PH), were chosen as raw materials. These materials were

ground and sieved, and the resulting 1 mm to 2 mm size fraction was used for the pyrolysis tests. In order to understand characteristics of the samples, proximate and ultimate analyses were conducted; results are listed in Table 1, based on ASTM D5373 criterion and GB212-91/GB212-84 criterion, respectively. X-ray fluorescence (XRF) analyses were also conducted to determine the composition of ash in all samples. The XRF analyses of the samples are given in Table 2.

Table 1. Proximate and Ultimate Analyses of Samples (%)

Sample	Proximate analysis				Ultimate analysis				
	FC_d	A_d	V_d	M_d	C_d	H_d	O_d	N_d	S_d
AC	70.43	14.69	13.54	1.34	75.23	2.5	1.01	0.93	0.85
PS	16.39	0.45	77.95	5.21	48.04	5.6	39.77	0.37	0.06
WS	18.05	5.13	72.26	4.56	47.88	6.1	40.50	0.31	0.21
CB	17.82	1.98	74.66	5.54	45.33	3.7	43.31	0.46	0.14
PH	30.69	3.96	59.98	5.37	47.89	5.6	41.32	0.49	0.36

Note: FC, V, A, and M are fixed carbon, volatile, ash and moisture content respectively;All the measurement is performed in dry basis.

Table 2. Composition of Ash Obtained from Different Samples by XRF Analyses (%)

Sample	Ash Composition						
	SiO_2	Al_2O_3	Fe_2O_3	CaO	MgO	Na_2O	K_2O
AC	36.54	20.57	15.93	16.34	1.45	0.59	0.91
PS	43.21	8.76	4.31	18.82	2.76	1.68	7.90
WS	31.85	0.78	0.89	15.10	4.56	0.32	29.63
CB	24.87	1.92	2.21	3.92	0.99	0.43	51.20
PH	33.09	8.11	5.50	35.41	2.85	1.34	7.22

Char Preparation and Char Gasification

Char preparation and char gasification tests were carried out using a tube resistance furnace (TRF) and a thermo-balance. The chars were prepared by heating the samples from room temperature to 800 °C, 900 °C, 1000 °C, and 1100 °C, respectively, with a 20 °C/min heating rate under N_2 protection (120 mL/min). The target temperature then was held for 60 min. The samples were cooled subsequentially to room temperature under protection of N_2 and then carefully crushed into fine powder in an agate mortar. The particle size of less than 0.074 mm was sieved out for the subsequent tests.

Upon the completion of the char preparation, chars were continuously gasified on an HCT-3 thermo-balance to obtain the weight loss curve at atmospheric pressure. A 5 mg sample was charged into a corundum crucible and put into the thermo-balance; the sample was then heated from room temperature to reaction temperature (850 °C, 900 °C, 950 °C, and 1000 °C) at a constant heating rate 20 °C/min under N_2 (100 mL/min), while keeping the temperature constant for 5 min. After that, CO_2 (100 mL/min, 99.999%) was supplied as the gasifying agent; all test runs were conducted until weight loss was completed. To check the reproducibility, each test was repeated at least three times before a final result was obtained.

Char conversion (X) and gasification reactivity (r,s^{-1}) were calculated by the following equations (Eqs. 1 and 2),

$$X = \frac{(m_0 - m_t)}{(m_0 - m_{ash})} \quad (1)$$

$$r = \frac{dX}{dt} \quad (2)$$

where m_o denotes the sample mass at the start of the gasification, m_t is the sample mass at gasification time t, and m_{ash} is the mass of ash remained after complete gasification.

RESULTS AND DISCUSSION

Effect of Pyrolysis Temperature on Char Characterization

Considering the influence of pyrolysis temperature on the performance of gasification, peanut hull char (PH-char) as a representative was selected in this section to study the effect of pyrolysis temperature on char characterization.

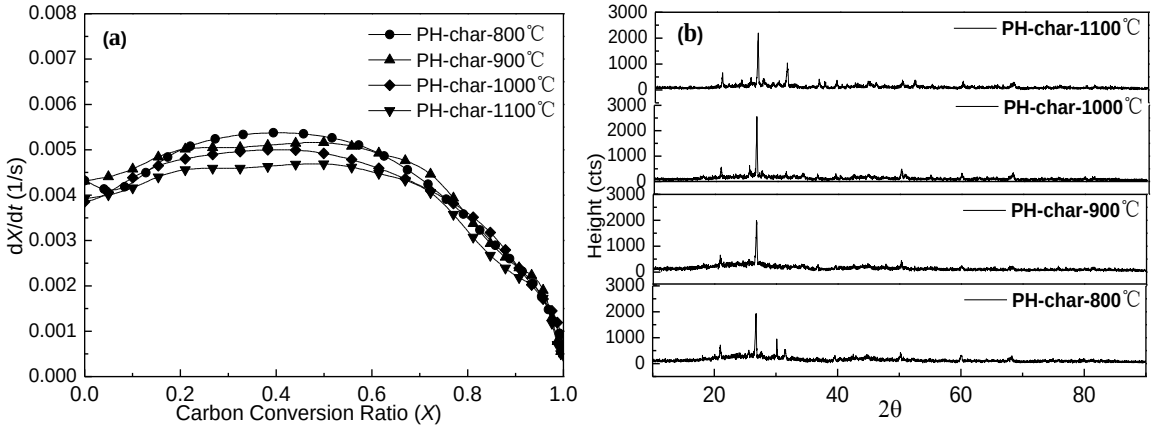

Fig. 1. (a) dX/dt versus X curves of chars gasified at 1000 °C, and (b) XRD pattern of the PH-char pyrolyzed at different temperatures

Figure 1(a) shows the reaction rate (dX/dt) at four pyrolysis temperatures for the preparation of PH-char to be gasified at 1000 °C. This figure indicates that PH-char pyrolysis at 1100 °C exhibited the lowest reaction rate, and the reaction rate increased with the decrease of pyrolysis temperature. Philips X'Pert MPD XRD was employed to investigate the effect of temperature on carbon chemical structure. One gram char samples with particle size of less than 0.074 mm were scanned from 10° to 90° at 10°/min scanning rate. The results are shown in Fig. 1(b). Diffraction peaks were observed in all the char samples at $2\theta \approx 26°$, corresponding to the (002) band. The (002) band of carbon is attributed to the stacking structure of aromatic layers. To obtain quantitative information of char structure from the XRD analysis, X'Pert High Score Plus software (PANalytical B.V., Netherlands) was used to process the XRD raw data. The crystal plane distance (d_{002}) was calculated using the Bragg formulation (Bragg 1913), while crystal stacking heights (L_c) of the chars were calculated through the Scherrer formula (Patterson 1939). The d_{002}/L_c values of PH-char pyrolysis at 800 °C, 900 °C, 1000 °C, and 1100 °C were 0.03472/1.07, 0.03471/1.28, 0.03457/1.54, and 0.03453/1.60, respectively, as shown in

Fig. 2. The d_{002} values decreased and L_c values increased with a rise in pyrolysis temperature, suggesting that the stacking structure is developing, crystallite size is increasing, defects are being removed, amorphous carbon structures number is decreasing, and carbon structure ordering is increasing (Yuan *et al*. 2012). The results indicate that non-carbon atoms are progressively being detached from biomass and coal with the increase of char preparation temperature. When the char preparation temperature was held at 1100 °C for 60 min, the volatile content in char was quite low, and the structure of the char tended to be in order. Therefore, the potential impact of residual volatile content and carbon structures in chars caused by different gasificatioin temperature schemes on char gasification reaction is considered as negligible when char is prepared under this condition. So all char samples used in following gasification experiments are those prepared at 1100 °C in order to reveal the inherent gasfication reaction behavior.

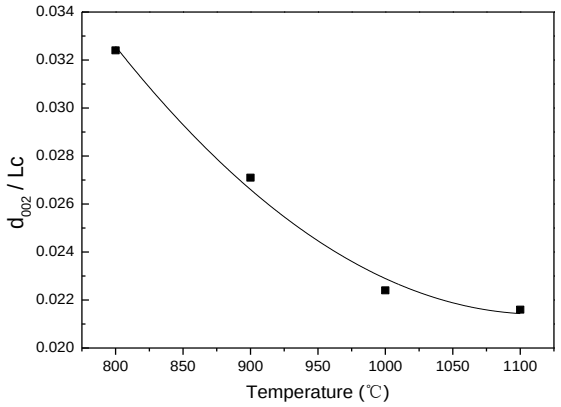

Fig. 2. The values of d_{002}/Lc at different pyrolysis temperature

Reactivity of Different Chars

Gasification rates of five chars derived from pyrolysis at 1100 °C are shown in Fig. 3 (a-e), with the gasification temperature ranging from 850 °C to 1000 °C. The reaction rates of char gasification for all five chars first increased and then decreased after reaching the peak value during the gasification process. The observed trend of the reaction rate can be explained with a changing specific surface area resulting from the degree of reaction proceeding. At the beginning stage of reaction, the porosity and size of char apertures keep growing, leading to a rise in specific surface area. With the reaction proceeding further, the pore wall thickness reduce to the threshold, then the pores collapse and merge, and in turn the specific surface area begins to decrease (Yan *et al*. 2014). Thus the gasification reaction rate shows a trend of decrease following the initial increase. The maximum reaction rates of five kinds of char gasification at different gasification temperatures are shown in Fig. 3 (f). The result indicates that gasification reactivity is a function of gasification temperature and increases with gasification temperature rise. At the same temperature, gasification reactivities of five chars can be ranked as CB-char>WS-char>PH-char>PS-char>AC-char. In general the difference in gasification reaction rate can be attributed to a combined effect of volatile content, particle size, pore structure, and mineral type and content. Given that the biomass pyrolysis temperature is held at 1100 °C for 60 min and the volatile content is very low, the content of volatile matter is not the major factor influencing the maximum gasification rate of chars .

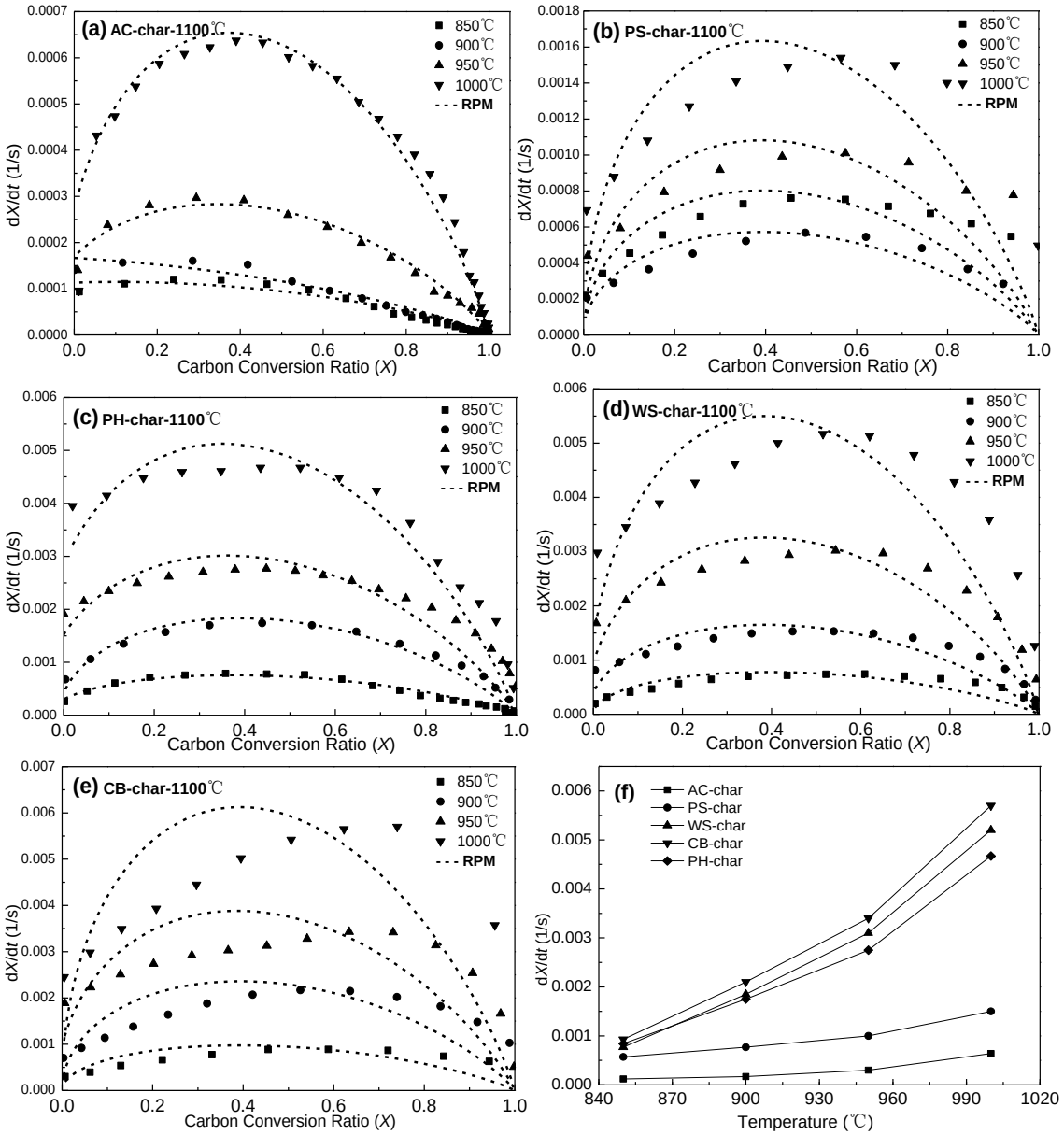

Fig. 3. (a-e) Different char reactivity curves as a function of temperature and fitted to the RPM model with carbon conversion ratio, and (f) the maximum reaction rate of char gasification

The size distribution of char samples with particle size less than 0.074 mm was analyzed with laser particle size analyzer. As shown in Fig 4, the particle size distributions of different chars were found to be very similar, ranging between 0.01 and 0.10 mm. The order of particle size for various chars could be ranked as PS-char>AC-char>PH-char>WS-char>CB-char. It is widely believed that the smaller the particle size of samples and the bigger the specific surface area, the faster will be the reaction rates. However, when comparing the reaction performance of the five different samples, there was no corresponding relationship between the particle size and gasification reactivity. Therefore, it can be concluded that the particle size of these five chars was not the determining factor influencing the gasification rate.

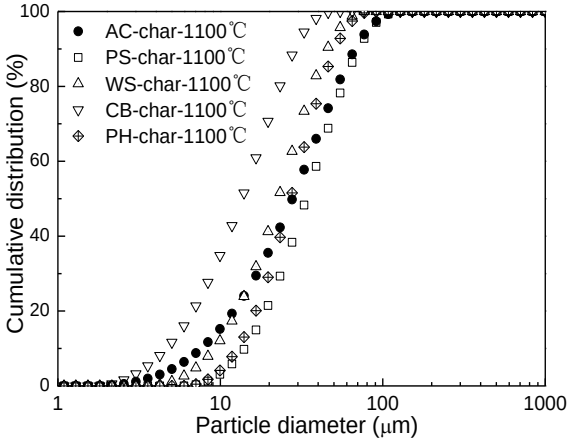

Fig. 4. Particle size distributions of chars

The specific surface area of the sample is dependent not only on particle size of the sample, but also on the pore structure as well as the number of holes in the sample. In this study, a scanning electron microscope and nitrogen adsorption specific surface area tester were also employed to analyze the microstructure and specific surface area of samples. The SEM pictures and the specific surface areas of AC-char, PS-char, WS-char, and CB-char pyrolysis at 1100 °C are presented in Fig. 5. The results show that the AC-char-1100 °C particles presented a wider granularity scale, and a relatively more compact structure. Based on the results, the specific surface area of the coal char was lower than all biomass chars, indicating that the coal char structure was denser, and it had lower porosity. Thus this result can explain why the coal char had the lowest gasification reaction rate. In addition, PS-char-1100 °C had a plate-like shape, and it was difficult to identify large pores in its particles. PH-char-1100 °C, WS-char-1100 °C, and CB-char-1100 °C particles had a porous and loose structure. Meanwhile, Fig 5(f) presents that WS-char had the greatest specific surface area and CB-char had lower specific surface area, which is inconsistent with the fact that CB-char had better gasification reactivity than WS-char. Therefore, the specific surface area and pore structure of these five chars were not the main factors influencing the gasification rate in this test.

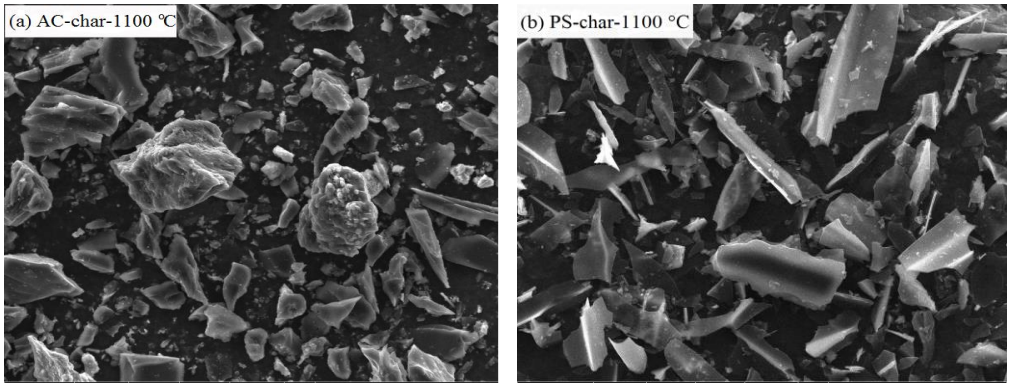

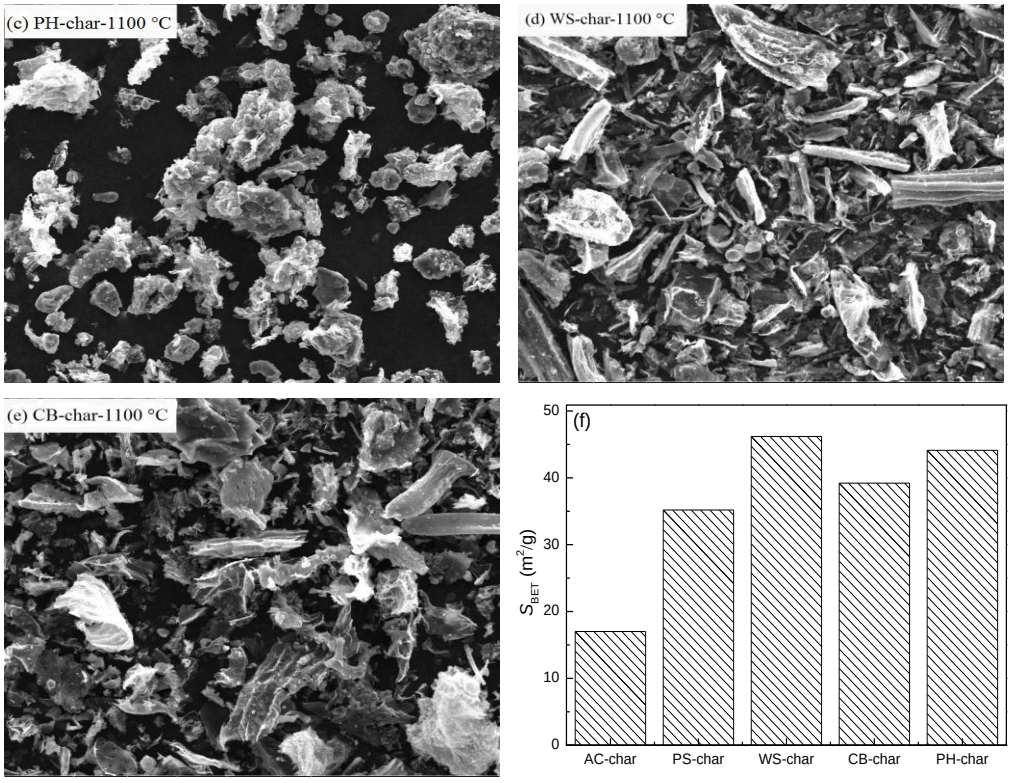

Fig. 5. (a-e)SEM of different chars derived at 1100 °C (1000x), and **(f)** The S_{BET} of different chars

It is well understood that the gasification reactivity of carbonaceous materials in the char can be markedly enhanced in the presence of alkali metal. A mechanism was proposed (Wigmans *et al.* 1983) to explain the reactivity pattern during alkali metal carbonate-catalyzed gasification of activated carbon in steam. The same mechanism may be applied to CO_2 gasification according to the following reaction (Eq. 3):

$$2MC_x + CO_2 \rightarrow M_2O + CO + 2C_x \quad (3)$$

The catalyst M_2O is trapped in an intercalated structure and plays an active role in a redox cycle. Also, the amount of M_2O will increase with progressing carbon gasification, which provides a condition under which the active sites are increased and the reaction rate is promoted. Some reaserchers (Sakawa *et al.* 1982; Kim *et al.* 2011) proposed an alkali ratio (AR) to quantify the catalytic activity of minerals on the basis of modified alkali index, which has elminated the ash content influence, caused by diffusion resistance when CO_2 penetrates and diffuses into the char surface through a thick blanket of ash. The alkali ratio is defined as the ratio of the sum of the mole fractions of the alkali compounds to the sum of the mole fractions of the acid compounds in the ash:

$$\text{Alkali ratio} = \frac{Fe_2O_3 + CaO + MgO + Na_2O + K_2O}{SiO_2 + Al_2O_3} \quad (4)$$

Figure 6 shows the measured alkali ratio of chars. A good correlation was found between the reactivity and the alkali ratio. So the alkali ratio of chars can be regarded as an important factor to evaluate gasification reactivities of different chars. A similar result was reported by Huang *et al.* (2009) regarding the effects of metal catalysts on CO_2 gasification reactivity of biomass char.

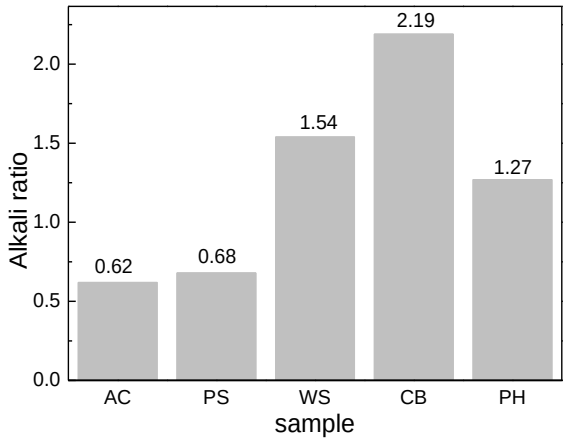

Fig. 6. Alkali ratio of chars

Kinetic Analysis

To evaluate the reactive behavior of chars during the CO_2 gasification process, the random pore model (RPM) (Bhatia and Perlmutter 1980) was applied in which the reaction rate is expressed as,

$$\frac{\mathrm{d}X}{\mathrm{d}t} = k_{\mathrm{RPM}}\left(1-X\right)\sqrt{1-\psi\ln\left(1-X\right)} \tag{5}$$

where, k_{RPM} is the reaction rate constant, and ψ is a structural constant related to the initial pore structure of the char sample (X=0).

$$\psi = \frac{4\pi L_0\left(1-\varepsilon_0\right)}{S_0^2} \tag{6}$$

In Eq. 6, S_0, L_0 and ε_0 are the pore surface area, pore length, and solid porosity, respectively.

The applicability of the RPM kinetic model to describe the gasification rate of different chars at various temperatures is presented in Fig. 3 (a-e). It can be found that the RPM could describe the char gasification behavior in most situations except PS-char-1100 °C, WS-char-1100 °C, and CB-char-1100 °C gasified at high temperature. Taking gasification rates at a conversion of 0.5 ($r_{0.5}$) as the basis, $\ln k_{0.5}$ versus $1/T$ is plotted in Fig. 7, and the activation energy (E_a) and the pre-exponential factor(A) were obtained by a linear regression with the data given in Table 4. A report (Kim *et al*. 2011) confirmed that mass transfer, which includes both the external diffusion through the bed of char particles and the internal diffusion inside the pores of the single particle, is negligible, and the gasification rate is controlled by chemical reactions when the reaction rate is less than 0.0082 s^{-1}. In this study, the maximum gasification reaction rate was 0.0059 s^{-1} at PH-char-1100 °C and gasified at 1100 °C. Therefore, the gasification reaction of char in this study was controlled by the chemical reaction. Table 3 shows that E_a was reduced to 217.1 kJ/mol for AC-char-1100 °C, while E_a was reduced to 152.4 kJ/mol, 150.7kJ/mol, 147.5 kJ/mol, and 142.6 kJ/mol for PS-char-1100 °C, PH-char-1100 °C, WS-char-1100 °C, and CB-char-1100 °C, respectively. It is consistent with the results from Fig. 3(f) that CB-char-1100 °C had the highest reactivity, followed by WS-char-1100 °C, PH-char-1100 °C, PS-char-1100 °C, and AC-char-1100 °C.

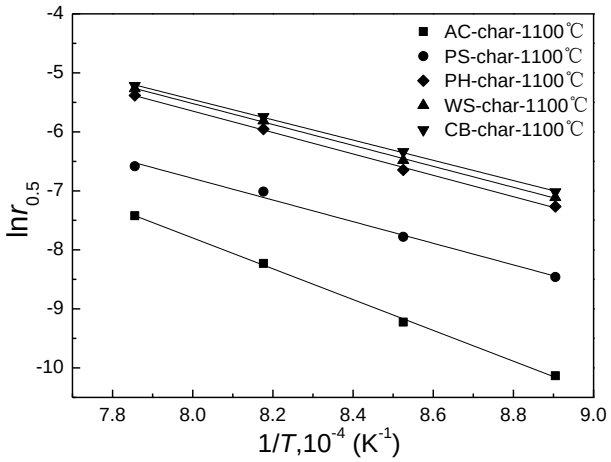

Fig. 7. Arrhenius plots for different char gasification reactions

Table 3. Apparent Activation Energy (E_a) and Frequency Factors (A)

Char	E_a (kJ/mol)	A (1/s)
AC-char-1100 °C	217.1	4.83E+05
PS-char-1100 °C	152.4	2.62E+03
PH-char-1100 °C	150.7	6.97E+03
WS-char-1100 °C	147.5	5.83E+03
CB-char-1100 °C	142.6	3.92E+03

The RPM model could well describe the AC-char-1100 °C gasification, where the maximum reactivity was at conversion levels of X<0.393. This is comparable to previous coal char gasification results (Kajitani *et al.* 2006). The RPM model also fit the experimental data well for PH-char-1100 °C, where the reactivity indicated a steady decrease with the increase of conversion. The RPM was established on the basis of characterized char reactivity by introducing a pore structure parameter to describle pore distribution. It essentially treats the reacting char as a pure carbon solid, in which the reaction surface is given by the internal surface of the uniform cylinders. However, neither the pore shape nor the purity of the solid in reality is perfect. In other words, the real chars from biomass generally contain a certain amount of minerals, which can cause deviations from the theory based on the absence of minerals. The result is that the original RPM did not predict the cases where there was a maximum reaction rate in the high conversion range X>0.6, as shown in PS-char-1100 °C, WS-char-1100 °C, and CB-char-1100 °C gasified at high temperature. An attempt has been made to modify the original random pore model for more extensive application (Zhang *et al.* 2014). The modified random pore model (MRPM) was made by introducing a new conversion term with one dimensionless parameter into the original random pore model, as indicated in Eq. 6,

$$\frac{\mathrm{d}X}{\mathrm{d}t} = k_{\mathrm{RPM}} (1 - X)^n \sqrt{1 - \psi \ln (1 - X)} \quad (6)$$

where, n is an empirical constant, which is influenced by the shape structure and porosity of solid reactant, and the presence of catalysts, and gas reactants. Figure 8 shows the applicability of the MRPM to the experimental results obtained from CO_2 gasification of different chars. This modified model could reasonably interpret the experimental results. The regression coefficients (R^2) and the kinetic constants of the model fitting to the

experimental data are summarized in Table 4. With regard to the condition of Fig. 8, some researchers consider that the increase of the specific area, caused by pore collapse and development during gasification, was the reason (Marquez-Montesinosa *et al*. 2002). However, other researchers believed that alkalis might be covered by some inert products during char preparation, and with the increasing conversion of char during gasification, these alkalis could be released and lead to high gasification rates in high conversion ranges (Wigmans *et al.* 1983). This could be the real reason for RPM's failure to predict the reactivities of the above biomass char.

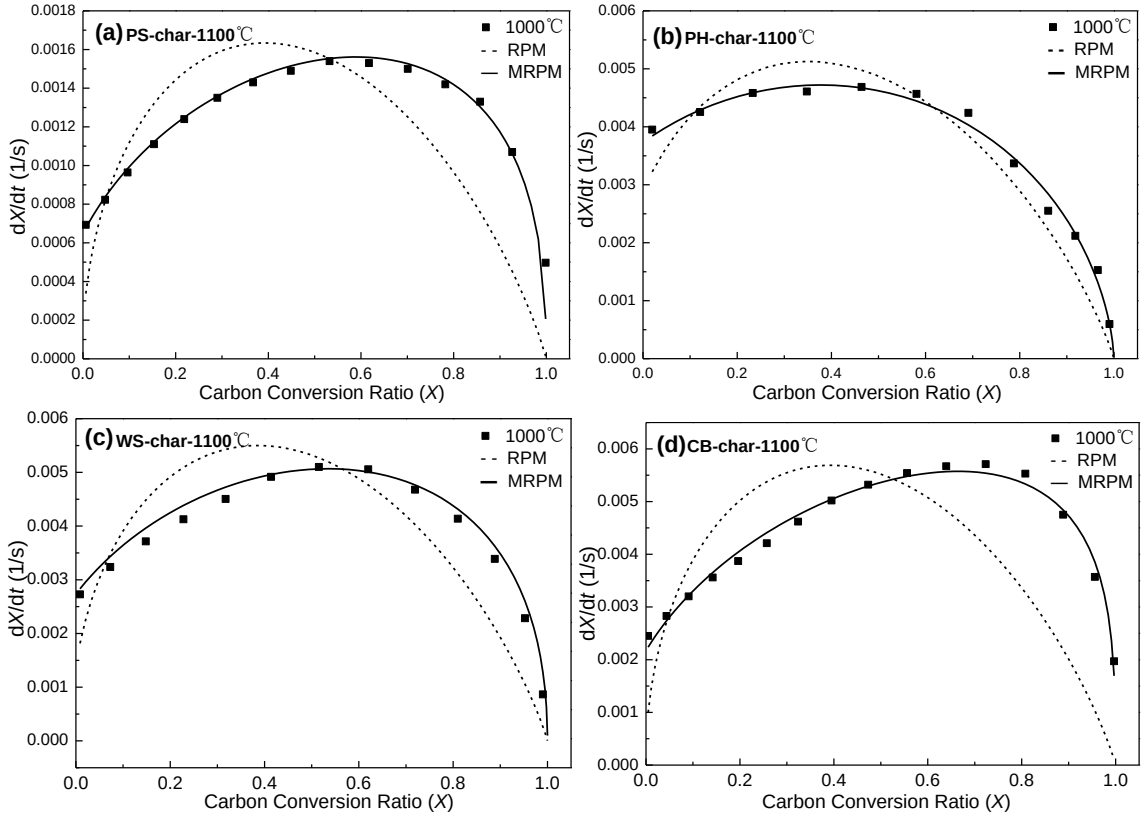

Fig. 8. Fitting result comparisons of MRPM and RPM on gasification rates of biomass char: (a) PS-char, (b) PH-char, (c) WS-char, and (d) CB-char

Table 4. Fitting Parameters of M-RPM and Shifted M-RPM

Sample	*A* (1/s)	ψ	*n*	R^2
PS-char	1.92E+03	15.45	0.52	0.9817
PH-char	1.65E+03	4.61	0.72	0.9896
WS-char	1.78E+03	9.48	0.57	0.9955
CB-char	1.84E+03	14.00	0.46	0.9854

Note: The temperature of char samples gasification was 1100 °C.

CONCLUSIONS

1. The char type has a significant impact on gasification reactivity. Based on results of the present study, biomass char is superior to that of anthracite char with respect to gasification reactivity. The gasification reactivities of the five studied chars can be ranked as CB-char>WS-char>PH-char>PS-char>AC-char. Char reactivity has a good

correlation with the alkali ratio (AR), which can quantify the catalytic effect of alkali in the mineral.

2. RPM can describe most of the char gasification phenomenon, except for biomass char (PS-char-1100 °C, WS-char-1100 °C, and CB-char-1100 °C) gasified at high temperatures. The RPM was modified and applied to these catalytic gasification systems, and it was found that the MRPM predicts the experimental reactivity satisfactorily.

ACKNOWLEDGEMENTS

The present work was supported by National Science Foundation of China (No. 51104014) and National Science Foundation of China & Baosteel under Grant (51134008).

REFERENCES CITED

Ahn, D. H., Gibbs, B. M., Ko, K. H., and Kim, J. J. (2001). "Gasification kinetics of an Indonesian subbituminous coal-char with CO_2 at elevated pressure," *Fuel* 80, 1651-1658. DOI: 10.1016/S0016-2361(01)00024-2

Barea, A. G., Vilches, L. F., Leiva, C., Campoy, M., and Pereira, C. F. (2009). "Plant optimisation and ash recycling in fluidised bed waste gasification," *Chemical Engineering Journal* 146(2), 227-236. DOI: 10.1016/j.cej.2008.05.039

Bhatia, S. K., and Perlmutter, D. D. (1980). "A random pore model for fluid-solid reactions: I. Isothermal, kinetic control," *AIChE Journal* 26(3), 379-386. DOI: 10.1002/aic.690260308

Bragg, W. L. (1913). "The diffraction of short electromagnetic waves by a crystal," *Proceedings of the Cambridge Philological Society* 17, 43-57.

Chen, T. J., Wu, J. L., Zhang, J. Z., Wu, J. H., and Sun, L. (2013). "Gasification kinetic analysis of the three pseudocomponents of biomass-cellulose, semicellulose and lignin," *Bioresource Technology* 153, 223-229. DOI: 10.1016/j.biortech.2013.12.021

Chouchene, A., Jeguirim, M., Favre-Reguillon, A., Trouvé, G., Le Buzit, G., and Khiari, B. (2012). "Energetic valorisation of olive mill wastewater impregnated on low cost absorbent: sawdust versus olive solid waste," *Energy* 39, 74-81. DOI: 10.1016/j.energy.2011.03.044

Demirbas, A. (2005). "Potential applications of renewable energy sources, biomass combustion problems in boiler power systems and combustion related environmental issues," *Progress in Energy and Combustion Science* 31(2), 171-192. DOI: 10.1016/j.pecs.2005.02.002

Dorge, S., Jeguirim, M., and Trouve, G. (2011). "Thermal degradation of Miscanthus pellets: kinetics and aerosols characterization," *Waste and Biomass Valorization* 2, 149-55. DOI: 10.1007/s12649-010-9060-4

Gunarathne, D. S., Mueller, A., Fleck, S., Kolb, T., Chmielewski, J. K., Yang, W. H., and Blasiak, W. (2014). "Gasification characteristics of steam exploded biomass in an updraft pilot scale gasifier," *Energy* 71(15), 496-506. DOI: 10.1016/j.energy.2014.04.100

Hognon, C., Dupont, C., Grateau, M., and Delrue, F. (2014). "Comparison of steam gasification reactivity of algal and lignocellulosic biomass: Influence of inorganic elements," *Biomass Techology* 164, 347-353. DOI: 10.1016/j.biortech.2014.04.111

Huang, Y. Q., Yin, X. L., Wu, C. Z., Wang, C. W., Xie, J. J., Zhou, Z. Q., Ma, L. L., and Li, H. B. (2009). "Effects of metal catalysts on CO_2 gasification reactivity of biomass char," *Biotechnology Advances* 27(5), 568-572. DOI: 10.1016/j.biotechadv.2009.04.013

Huo, W., Zhou, Z. J., Wang, F. C., Wang, Y. F., and Yu, G. S. (2014). "Experimental study of pore diffusion effect on char gasification with CO2 and steam," *Fuel* 131, 59-65. DOI: 10.1016/j.fuel.2014.04.058

Jeong, H. M., Seo, M. W, Jeong, S. M., Na, B. K., Yoon, S. J., Lee, J. G., and Lee, W. J. (2014). "Pyrolysis kinetics of coking coal mixed with biomass under non-isothermal and isothermal conditions," *Bioresource Technology* 155, 442-5. DOI: 10.1016/j.biortech.2014.01.005

Kajitani, S., Suzuki1, N., shizawa, M., and Hara, S. (2006). "CO_2 gasification rate analysis of coal char in entrained flow coal gasifier," *Fuel* 85(2), 163-169. DOI: 10.1016/j.fuel.2005.07.024

Kim, Y. T., Seo, D. K., and Wang, J. H. (2011). "Study of the effect of coal type and particle size on char-CO_2 gasification via gas analysis," *Energy & Fuels* 25(11), 5044-5054. DOI: 10.1021/ef200745x

Mani, T., Mahinpey, N., and Murugan, P. (2011). "Reaction kinetics and mass transfer studies of biomass char gasification with CO_2," *Chemical Engineering Science* 66(1), 36-41. DOI: 10.1016/j.ces.2010.09.033

Marquez-Montesinosa, F., Corderob, T., Rodríguez-Mirasolb, J., and Rodríguez, J. J. (2002). "CO_2 and steam gasification of a grapefruit skin char," *Fuel* 81(4), 423-429. DOI: 10.1016/S0016-2361(01)00174-0

Masnadi, M. S., Habibi, R., Kopyscinski, J., Hill, J. M., Bi, X. T., Lim, J. (2014). "Fuel characterization and co-pyrolysis kinetics of biomass and fossil fuels," *Fuel* 117, 1204-14. DOI: 10.1016/j.fuel.2013.02.006

McKendry, P. (2002b). "Energy production from biomass (part 2): conversion technologies," *Bioresource Technology* 83, 47-54. DOI: 10.1016/S0960-8524(01)00119-5

Patterson, A. (1939). "The Scherrer formula for X-ray particle size determination," *Physical Review* 56(10), 978. DOI: 10.1103/PhysRev.56.978

Rapagna, S., Jand, N., Kiennemann, A., and Foscolo, P. U. (2000). "Steam-gasification of biomass in a fluidised-bed of olivine particles," *Biomass and Bioenergy* 19(3), 187-197. DOI: 10.1016/S0961-9534(00)00031-3

Richardson, Y., Tanoh, S. T., Julbe, A., and Blin, J. (2015). "Improving the kinetics of the CO2 gasification of char through the catalyst/biomass integration concept," *Fuel* 154(15), 217-221. DOI: 10.1016/j.fuel.2015.03.059

Sakawa, M., Sakurai, Y, and Hara, Y. (1982). "Influence of coal characteristics on CO_2 gasification," *Fuel* 61(8), 717-720. DOI: 10.1016/0016-2361(82)90245-9

Wang, G. W., Zhang, J. L., Hou, X. M., Shao, J. G., and Geng, W. W. (2014). "Study on CO_2 gasification properties and kinetics of biomass chars and anthracite char," *Bioresource Technology* 177, 66-73. DOI: 10.1016/j.biortech.2014.11.063

Wigmans, T., Gebel, J. C., and Moulij, J. A. (1983). "The influence of pretreatment condition on the activity and stability of sodium and potassium catalysts in carbon–steam reactions," *Carbon* 21(3), 295-301. DOI: 10.1016/0008-6223(83)90094-5

Wu, S., Gu, J., Li. L., Wu, Y., Gao, J. (2006). "The Reactivity and Kinetics of Yanzhou Coal Chars from Elevated Pyrolysis Temperatures During Gasification in Steam at 900-1200 °C," Process Safety and Environmental Protection 84(6), 420-428. DOI: 10.1205/psep06031

Yan, Q. X., Huang, J. J.,Zhao, J. T., Li, C. Y., Xia, L. S., and Fang, Y. T. (2014). "Investigation into the kinetics of pressurized steam gasification of chars with different coal ranks," *Journal of Thermal Analysis and Calorimetry* 116(1), 519-527. DOI: 10.1007/s10973-013-3492-6

Yuan, S., Dai, Z., Zhou, Z., Chen, X., Yu, G., and Wang, F. (2012). "Rapid co-pyrolysis of rice straw and a bituminous coal in a high-frequency furnace and gasification of the residual char," *Bioresource Technology* 109, 188-197. DOI: 10.1016/j.biortech.2012.01.019

Zhang, J. L., Wang, G. W., Shao., J. G., and Zuo, H. B. (2014). "A modified random pore model for the kinetics of char gasification," *BioResources* 9(2), 3497-3507.

Zou, J. H., Zhou, Z. J., Wang, F. C., Zhang, W., Dai, Z. H., Liu, H. F., and Yu, Z. H. (2007). "Modeling reaction kinetics of petroleum coke gasification with CO2," *Chemical Engineering and Processing* 46, 630-636. DOI: 10.1016/j.cep.2006.08.008

Article submitted: January 23, 2015; Peer review completed: April 25, 2015; Revisions accepted: June 16, 2015; Published: July 3, 2015.
DOI: 10.15376/biores.10.3.5242-5255